Comprehensive Study on the Structural, Electrical, and Thermistor Behaviour of Sodium Manganese Titanium Tungstate Ceramic

S B Bhoobash[1], M Suman Kalyan[1] and C Behera [1,2,*]

1 Advanced Functional Materials Research Laboratory, Department of Physics, National Institute of Technology, Agartala, Tripura - 799046, India.
2 Physics Section, DESM, Regional Institute of Education (NCERT), Bhopal, Madhya Pradesh - 462013, India.
*Corresponding Author - cdbehera1986@gmail.com, chakradhar.b@ncert.nic.in

Abstract. A mixed B-site double perovskite ceramic, $Na_2(Mn_{0.5}Ti_{0.5})WO_6$, was synthesised via a conventional solid-state route and comprehensively examined for its structural, microstructural, dielectric, impedance, and thermistor properties. X-ray diffraction analysis confirmed that the ceramic exhibits a dual-phase crystal structure. FESEM imaging revealed densely packed agglomerated grains with an average size of ~220 nm, while EDX confirmed the homogeneous distribution of Na, Mn, Ti, W, and O without extraneous impurities. Dielectric studies showed strong frequency-dependent dispersion and an increase in permittivity with temperature, attributed to Maxwell–Wagner interfacial polarisation and thermally activated defect dynamics. Impedance spectroscopy demonstrated non-Debye relaxation and revealed that the grain- and grain-boundary-related contributions evolve with temperature, consistent with a transition from (CQR) to (CQR)(CR) circuit behaviour. Measurements of resistance that depend on temperature showed a clear negative-temperature-coefficient (NTC) thermistor response that was caused by small-polaron hopping and conduction through oxygen vacancies. The results taken together show that the ceramic is a good choice for use in electronics and high-temperature sensing.

Keywords: Double Perovskite, XRD, Dielectric, Impedance, Thermistor.

1 Introduction

In recent years, the search for advanced functional ceramics has become more intense. This is because there is a growing need for materials that can support next-generation technologies in energy storage, optoelectronics, sensing, and information systems. Complex perovskites, especially double perovskites, are some of the most flexible candidates among the different oxide families. Their natural ability to change shape and the fact that their electrical, magnetic, optical, and thermal responses can be easily

J. Saxena et al. (eds.), *Proceedings of the International Conference on Sustainable Micro-Nano Materials & Innovative Technology (ICSUMMIT 2026)*, Atlantis Highlights in Engineering 44,
https://doi.org/10.2991/978-94-6239-727-9_2

changed make them a major focus of current materials research [1,2]. The ordered addition of two different cations at the B-site sets double perovskites apart from the usual ABO_3 structure. This feature gives engineers a powerful way to change the electronic structure and the chemistry of defects. You can fine-tune charge transport, polarisation mechanisms, and local symmetry with this flexible composition. Adding transition-metal ions with different oxidation states makes the landscape even more interesting by causing controlled lattice distortions, octahedral tilting, and strong electronic correlations. These are also the same properties that make them useful in optical components, photovoltaics, memory elements, spintronic devices, and electrocatalysts [3–5].

Because they have strict requirements for ionic radius and charge balance, sodium-based A^{1+} double perovskites are a smaller group within this larger family. But they have become very popular in the last few years. The limited B-site valence combinations that are allowed in $A_2BB'O_6$ compositions (like B'^{5+}/B''^{5+} or B'^{4+}/B''^{6+}) put strict chemical limits on the compositions. But these limitations give researchers a chance to look more closely at compositions that have better structural stability and customised functions [6,7]. One of the best things about double perovskites is that they can hold different cations at both the A and B sites. This causes a lot of different structural behaviours, such as long-range order, local distortions, and even the creation of multiple phases. These structural changes often happen because of differences in ionic radii, rules that say charges must be neutral, or different thermodynamic phases [8]. This kind of complexity can change the phase purity, but it can also improve the material's performance. Microstructural properties, such as the shape of the grains, the properties of the grain boundaries, and the types of defects, are very important in determining dielectric response, conduction pathways, and relaxation mechanisms. In the end, double perovskites are great candidates for future ceramic-based electronic and thermal-sensing technologies because they can change their structure, have a lot of different microstructures, and do more than one thing at once [9].

In this context, the mixed B-site engineered double perovskite $Na_2(Mn_{0.5}Ti_{0.5})WO_6$ emerges as a promising lead-free functional ceramic. Adding both Mn^{4+} and Ti^{4+} to the B-site of the $Na_2(B)WO_6$ framework at the same time is expected to cause big changes in the lattice because of ionic radius mismatch and charge compensation effects. The incorporation of mixed B-site occupancy constitutes a significant novelty of the present study, distinguishing it from previously reported double perovskite systems. This type of mixed occupancy can change the chemistry of defects by controlling how oxygen vacancies form, stabilising the structure that comes from perovskite, and changing how octahedra tilt [10]. The manuscript will refer to $Na_2(Mn_{0.5}Ti_{0.5})WO_6$ as NMTWO. This study focuses on the synthesis and comprehensive characterisation of NMTWO ceramic produced via the solid-state method, analysing its structural properties, microstructural growth, dielectric characteristics, impedance properties, and thermistor response in detail. This systematic analysis aims to assess its suitability for next-generation high-temperature electronic components, thermal sensors, and multifunctional device applications.

2 Experimental Procedure

Figure 1 shows how to make the NMTWO ceramic using the traditional solid-state reaction method with high-purity precursor oxides: Na_2CO_3, MnO_2, TiO_2, and WO_3. The oxides were weighed in stoichiometric amounts. We ground the mixed powders both dry and wet, using acetone as the milling medium to make sure they mixed evenly and the particles were all the same size. The mixture was heated to 1025 K for four hours to speed up solid-state diffusion and the first steps in making the double perovskite. The calcined powder was then ground up very finely, pressed into pellets with a KBr hydraulic press, and then sintered in air at 1025 K for 6 hours to make it dense enough and develop the microstructure so that it could be electrically characterised.
We used X-ray diffraction (XRD) on a Rigaku Ultima IV diffractometer with Cu Kα radiation ($\lambda = 1.5405$ Å) to look at the phase purity and crystal structure of the calcined powder at room temperature. We recorded diffraction patterns over a 2θ range of 20° to 80° to get the main reflections. To make high-quality electrodes, silver paste was put on the opposite sides of the sintered pellets. Then, the pellets were heated to make sure that the electrical contact was good. Using an impedance analyser (PSMN4L, Model 1735), we looked at the dielectric and electrical transport properties over a frequency range of 1 kHz to 1 MHz and a temperature range of 298 to 398 K. We used field-emission scanning electron microscopy (FESEM, ZEISS) to look at the surface morphology and energy-dispersive X-ray (EDX) spectroscopy attached to the FESEM unit to check the elemental composition and spatial uniformity. This method for systematic synthesis and characterisation made it possible to fully assess the NMTWO ceramic's structural properties, electrical response, and overall functional potential.

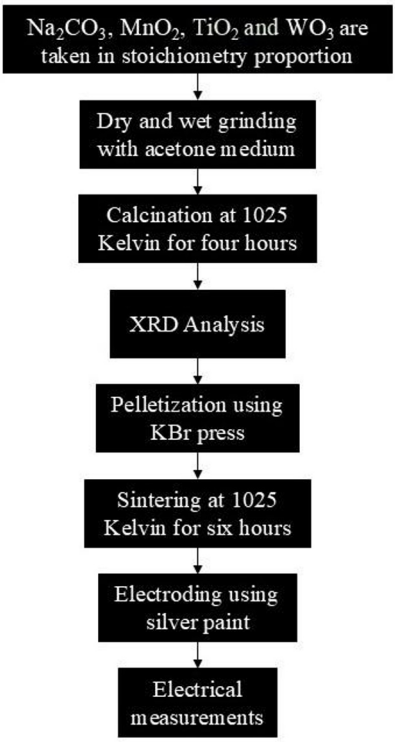

Fig. 1. Schematic representation of material synthesis in the solid-state method.

3 Results and Discussion

3.1 XRD Analysis

Figure 2 displays the X-ray diffraction (XRD) pattern of the calcined NMTWO ceramic across an extensive 2θ range (20°-80°). We used the X'Pert HighScore Plus software [11] to find the phases. The analysis indicates that the sample constitutes a stable solid solution comprised of two distinct phases. The primary diffraction peaks originate from the cubic Na_2WO_4 phase (Ref. code 01-070-1040), while the additional reflections are attributed to the monoclinic TiO_2 phase (Ref. code 00-046-1237) are marked with an asterisk (*). All reflections match known reference patterns, and there are no unknown peaks, which confirms that there are no impurity phases [12]. Having two phases in a material can change how well it works as a whole. The two phases could have different compositions, structures, or shapes, which is why this is the case. This kind of difference changes how things work mechanically, electrically, thermally, and chemically by adding processes like dispersion strengthening, precipitation hardening, and transformation toughening. In dielectric materials, the insulating and semiconducting phases can change the permittivity and loss characteristics. This makes it possible to change

the properties of the materials for use in electronics. In semiconductors, the coexistence of multiple phases can affect the mobility of charge carriers and the effectiveness of doping. These systems may undergo phase transformations that further affect functional behaviour and device performance [13] because phase stability depends on temperature and pressure.

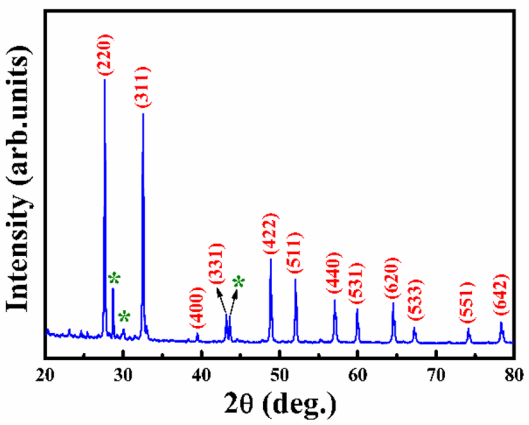

Fig. 2. XRD diffraction pattern of NMTWO ceramic.

3.2 SEM Analysis

The field-emission scanning electron microscopy (FESEM) image of the sintered surface of the NMTWO ceramic is shown in Figure 3a. The surface shows tightly packed agglomerated grains with very little visible porosity, which shows that solid-state sintering worked well and that the microstructure was well consolidated. The grains have uneven shapes and a wide range of sizes. This could be because Mn and Ti occupy different B-sites, which affects how the grains diffuse and grow during sintering [14]. Using ImageJ software [15], we found that the average grain size was 220 nm. Figure 3b shows the energy-dispersive X-ray (EDX) spectrum that goes with it. It shows that the elements Na, Mn, Ti, W, and O are present, and there are no extra peaks for impurities. This confirms that the NMTWO system that was made has pure composition and uniform elements.

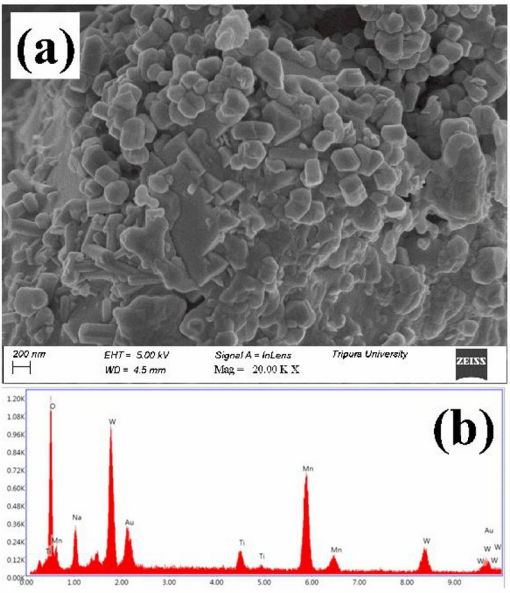

Fig. 3. (a) FESEM and (b) EDX spectrum of NMTWO ceramic.

3.3 Dielectric Study

We measured the NMTWO ceramic's dielectric permittivity (ε_r) and dielectric loss (tan δ) between 1 and 1000 kHz and at temperatures between 298 and 398 K to learn more about how it polarises and how it relaxes electrically. At all measured temperatures, εr slowly goes down as the frequency goes up, which is a common behaviour in mixed B-site transition-metal double perovskites. The elevated permittivity at low frequencies results from the capacity of electronic, ionic, dipolar, and interfacial polarisation processes to follow the applied field. At higher frequencies, slower polarisation mechanisms like space-charge and dipolar responses can't keep up with the oscillating field. This makes ε_r drop and eventually settle at higher frequencies, where only faster electronic and ionic contributions are important [16].

The measured range of ε_r changes a lot with temperature. ε_r goes up a lot as the temperature goes up. This is because the charge carriers are more thermally activated, which makes the polarisation at the grain boundaries stronger. The mixed occupancy of Mn and Ti at the B-site causes more lattice distortion and defect states. These states help space-charge build up and make the permittivity higher at higher temperatures. Figure 4b shows how the dielectric loss (tan δ) changes when the temperature and frequency change. Tan δ decreases with increasing frequency but rises with temperature, indicating thermally activated hopping conduction and defect-dipole relaxation. The higher loss values in the low-frequency region are attributed to grain boundary-dominated resistive behaviour. In contrast, the lower tan δ values at high frequencies confirm the ceramic's good insulating nature [17]. Overall, the frequency-dependent dispersion and

temperature-activated dielectric response demonstrate that NMTWO exhibits stable dielectric characteristics suitable for high-temperature electronic and sensing applications.

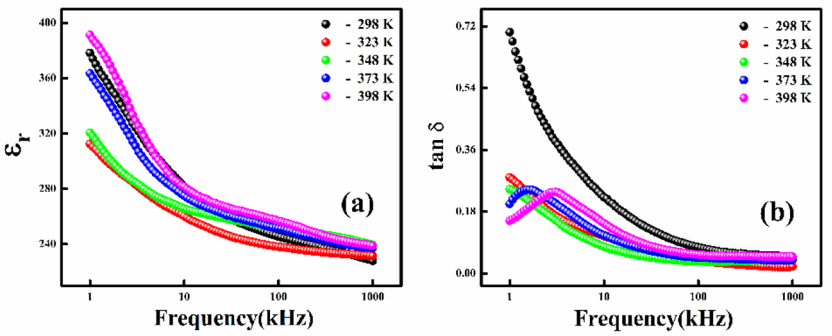

Fig. 4. (a) Dielectric permittivity and (b) tangent loss of NMTWO ceramic.

3.4 Impedance Study

The complex impedance spectra of NMTWO were analysed in the temperature range 298-398 K to elucidate the contribution of different microstructural regions to the electrical response. Figure 5 shows the Nyquist plots (Z″ vs. Z′), which exhibit depressed semicircular arcs whose diameters decrease with increasing temperature, indicating a substantial thermally activated reduction in resistance and confirming the ceramic's semiconducting nature. The non-ideal, tilted arcs suggest a distribution of relaxation times and therefore non-Debye-type relaxation behaviour [18]. The experimental data were modelled using ZsimpWin software [19]. In the lower temperature range (298-348 K), the impedance spectra were satisfactorily fitted using a (CQR) equivalent circuit, which includes a grain-related resistance element in parallel with a constant-phase component to account for distributed bulk capacitance. At higher temperatures (373-398 K), an additional contribution becomes evident, and the spectra are better described by a (CQR)(CR) circuit, where the second CR branch is associated with grain-boundary effects. The progressive emergence and strengthening of this additional arc with temperature signal enhanced grain-boundary conduction and space-charge accumulation at interfaces. The impedance analysis confirms that both grains and grain boundaries govern the electrical transport in NMTWO, with their resistances decreasing markedly with temperature due to thermally activated hopping of charge carriers.

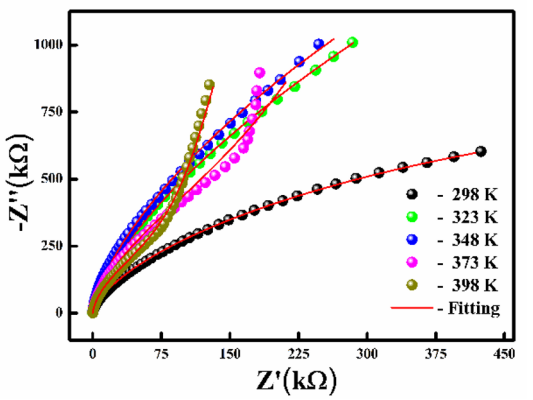

Fig. 5. Nyquist plot of NMTWO ceramic.

3.5 Thermistor Application

A thermistor is a temperature-dependent resistor whose electrical resistance changes predictably with temperature. Based on this behaviour, thermistors are classified as either negative temperature coefficient (NTC) or positive temperature coefficient (PTC) types. In NTC devices, resistance decreases with increasing temperature, whereas in PTC devices, resistance increases with rising temperature. In the present study, the NMTWO ceramic exhibits NTC-type behaviour, as evidenced by the monotonic decrease in resistance with increasing temperature (Figure 6).

$$\alpha = \left[\frac{1}{T_2 - T_1}\right]\left[\frac{R_2}{R_1} - 1\right] \quad (1)$$

$$\beta = \left[\ln\left[\frac{R_1}{R_2}\right]\right] \Big/ \left[\frac{1}{T_1} - \frac{1}{T_2}\right] \quad (2)$$

The resistance goes down a lot, from about 280 kΩ at 323 K to about 127 kΩ at 398 K. This shows that the material conducts electricity like a semiconductor. This decrease that depends on temperature shows that the electrical transport is mostly due to thermally activated hopping of small polarons, which is a well-known process in double perovskites made of transition metals. The computed temperature coefficient of resistance (α), thermistor constant (β) and activation energy (E_a) are given in Table 1 further validate the NTC characteristics of the compound. The β values are normal for oxide-based NTC ceramics, which means that the activation energies are moderate and good for use in thermal sensors [20]. The more negative α values at higher temperatures show that charge carriers can move more easily because thermal energy can break through localised trapping potentials.

There are several inherent factors that elucidate the behaviour of this material as NTC. The mixed occupancy of Mn and Ti on the B-site results in distinct oxidation states (Mn^{4+} and Ti^{4+}), facilitating polaronic hopping. Oxygen vacancies that happen during high-temperature sintering also create donor-type defect states, which help conduction

that is activated by thermal energy [21]. As the temperature rises, these carriers get more energy, which makes it easier for them to move between nearby transition-metal sites. This lowers the resistance a lot. Overall, the NMTWO ceramic shows stable, well-defined NTC behaviour across the temperature range we looked at. This shows that it could be used in temperature sensors, thermal monitoring devices, and other electronic parts where a predictable negative temperature dependence is important.

Table 1. Thermistor parameters and activation energy at different temperature ranges of NMTWO ceramic.

Parameters	α (K^{-1})	β (K)	E_a (eV)
323-348 K	-5.19×10^{-3}	625.39	0.0538
348-373 K	-1.05×10^{-2}	1573.19	0.1355
373-398 K	-1.21×10^{-2}	2130.50	0.1835

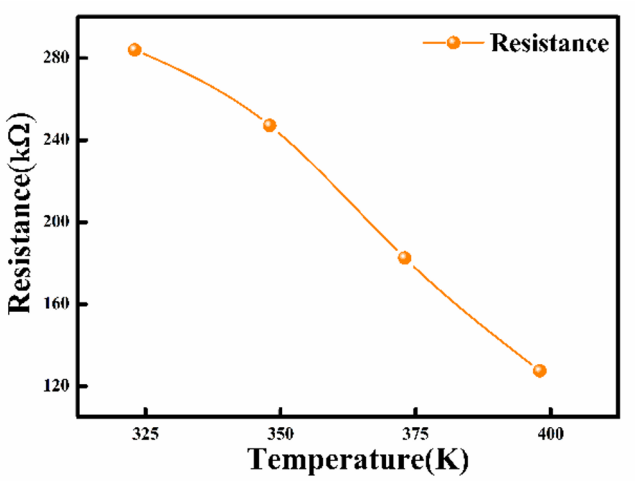

Fig. 6. Temperature-dependent resistance of NMTWO ceramic.

4 Conclusion

A thorough structural and electrical analysis of the NMTWO ceramic has been conducted to determine its suitability for functional device applications. The XRD analysis shows that the ceramic crystallises into a clear dual-phase solid solution with no detectable impurity phases. Microstructural observations showed that the nanoscale grains were tightly packed. EDX confirmed that the ions were pure and evenly spread throughout the material. The dielectric study showed that the frequency dispersion was strong and that the permittivity increased with temperature. These behaviours were caused by interfacial polarisation and defect-assisted hopping processes. Impedance spectroscopy further confirmed the simultaneous presence of grain and grain-boundary contributions, with equivalent-circuit modelling (CQR) at lower temperatures and (CQR)(CR) at

higher temperatures validating thermally activated conduction and non-Debye relaxation dynamics. The thermistor analysis showed a clear NTC-type response, with resistance steadily dropping across the temperature range that was looked at. This was because small-polaron hopping and oxygen-vacancy-driven charge transport were happening. Overall, the interplay of structural stability, favorable dielectric behaviour, well-defined impedance relaxation, and robust NTC characteristics positions NMTWO as a promising candidate for high-temperature sensors, thermal-monitoring elements, and multifunctional ceramic device components.

Acknowledgments. The authors thank SOA University for providing access to their XRD facility and Tripura University for granting access to their FESEM facility. This work is dedicated to the cherished memory of Prof. R. N. P. Choudhary. His invaluable guidance and enduring contributions will always be remembered. We extend our heartfelt condolences to his family.

Disclosure of Interest. The authors have no competing interests to declare that are relevant to the content of this article.

References

1. Sami, V., & Karppinen, M. (2015). $A_2B'B''O_6$ perovskites: A review. Progress in Solid State Chemistry, 43(1–2), 1–36. https://doi.org/10.1016/j.progsolidstchem.2014.08.001
2. Mishra, S., & Parida, S. K. (2023). An overview and recent progress in single- and double-perovskite metal oxides. In Perovskite metal oxides (pp. 55–80). Elsevier. https://doi.org/10.1016/B978-0-323-99529-0.00002-3
3. Bhalla, A. S., Guo, R., & Roy, R. (2000). The perovskite structure: A review of its role in ceramic science and technology. Materials Research Innovations, 4(1), 3–26. https://doi.org/10.1007/s100190000062
4. Bhoobash, S. B., Kalyan, S., Hota, S., Choudhary, R. N. P., & Behera, C. (2024). An investigation of the structure–property relation of Na_2MnWO_6 for device application. Inorganic Chemistry Communications, 169, 113048. https://doi.org/10.1016/j.inoche.2024.113048
5. Hossain, A., Bandyopadhyay, P., & Roy, S. (2017). An overview of double perovskites $A_2B'B''O_6$ with small ions at the A site: Synthesis, structure and magnetic properties. Journal of Alloys and Compounds, 740, 414–427. https://doi.org/10.1016/j.jallcom.2017.12.282
6. King, G., & Woodward, P. M. (2010). Cation ordering in perovskites. Journal of Materials Chemistry, 20(28), 5785–5796. https://doi.org/10.1039/B926757C
7. Bhoobash, S. B., & Behera, C. (2024). Exploring the unique structural, dielectric, and electrical properties of Na_2TiMoO_6 ceramic: A pioneering step towards advancing device applications. Ceramics International, 51. https://doi.org/10.1016/j.ceramint.2024.12.216
8. Ravi, S., & Senthilkumar, C. (2017). Room temperature multiferroicity in a new Ba_2FeMnO_6 double perovskite material. Ceramics International. https://doi.org/10.1016/j.ceramint.2017.07.217
9. Zhong, W.-M., Liu, Q.-X., Jiang, Y.-P., Deng, M.-L., Li, W.-P., & Tang, X.-G. (2021). Ultra-high dielectric tuning performance and double-set resistive switching effect achieved on the Bi_2NiMnO_6 thin film prepared by sol–gel method. Journal of Colloid and Interface Science. https://doi.org/10.1016/j.jcis.2021.08.109
10. Bhoobash, S. B., Kalyan, S., & Behera, C. (2025). Studies of the electrical and optical properties of sodium titanium tungstate ceramic for suitable electronic applications. Journal of

Materials Science: Materials in Electronics, 36. https://doi.org/10.1007/s10854-025-15981-8

11. Malvern Panalytical. (2017). X'Pert HighScore Plus (Version 4.8) [Computer software]. Malvern Panalytical B.V.
12. Jia, P., Zheng, Z., Li, Y., Li, Z., Tong, L., & Wang, Y. (2023). Achieving enhanced piezoelectric performance of KNN-based ceramics: Decisive role of multi-phase coexistence induced by lattice distortion. Journal of Alloys and Compounds, 930, 167416. https://doi.org/10.1016/j.jallcom.2022.167416
13. Liu, W., Wang, H., Hu, W., Du, Y., & Cheng, C. (2022). Understanding the origin of the high piezoelectric performance of KNN-based ceramics from the perspective of lattice distortion. Ceramics International, 48(7), 9731–9738. https://doi.org/10.1016/j.ceramint.2021.12.174
14. Goldstein, J., Newbury, D., Michael, J., Ritchie, N., Scott, J., & Joy, D. (2018). Scanning electron microscopy and X-ray microanalysis. Springer. https://doi.org/10.1007/978-1-4939-6676-9
15. Rasband, W. S. (1997–2018). ImageJ [Computer software]. U.S. National Institutes of Health.
16. Mishra, S., & Parida, S. (2023). Lead-free complex double perovskite $SrLiFeWO_6$: Structural, microstructure, electrical and optical study. Physica B: Condensed Matter, 668, 415246. https://doi.org/10.1016/j.physb.2023.415246
17. Das, R., & Choudhary, R. N. (2019). Structure, dielectric and electrical properties of relaxor lead-free double perovskite: Nd_2NiMnO_6. Processing and Application of Ceramics, 13, 1–11. https://doi.org/10.2298/PAC1901001D
18. Gerhardt, R. (1994). Impedance and dielectric-spectroscopy revisited: Distinguishing localized relaxation from long-range conductivity. Journal of Physics and Chemistry of Solids, 55, 1491–1506. https://doi.org/10.1016/0022-3697(94)90575-4
19. Boukamp, B. A. (2005). ZSimpWin (Version 3.21) [Computer software]. University of Twente.
20. Keskin, A. (2005). A simple analog behavioural model for NTC thermistors including self-heating effect. Sensors and Actuators A: Physical, 118, 244–247. https://doi.org/10.1016/j.sna.2004.06.034
21. Sahoo, S., Mishra, S., Sahoo, D., Parida, B. N., Biswal, L., & Parida, R. (2024). Dielectric, electric, and magnetic response of modified bismuth ferrite-based double perovskites for NTC-thermistor application. Ceramics International, 50. https://doi.org/10.1016/j.ceramint.2024.03.125